Chapter 5
The 1st August 2010 Solar Storm Effects on the Ionosphere in the Yangtze River Delta Region Based on Ground and Space GPS Technology

Hu Wang, Qian-xin Wang and Ying-yan Cheng

Abstract On 1st August 2010, the entire side of the sun facing earth erupted in a frenzy of solar activity. This solar storm just like a solar tsunami, the massive multiple filaments of magnetism were released from the solar surface during the solar storm. Then these high energy particles, protons and electrons from coronal mass ejections hit against the earth's magnetic field. These hits caused intensively geomagnetic storms and ionospheric variations. Now well established ground and space based GPS instruments can offer a unique chance for a real time monitoring of ionosphere variations and characteristics. So in this paper we investigate ionospheric behavior responded to the solar storm using Ground and Space based GPS measurements. Firstly this paper describes a method of real-time solving TEC and GPS instrumental biases using Kalman filtering, so this can be used to provide absolute amount of ionospheric TEC for real-time monitoring of ionosphere changes during the solar storm. The Yangtze River Delta regional ground based GPS network measurements are used and a real-time regional ionosphere model is created, then real-time VTEC and TEC rate are also calculated. Furthermore, in order to analyze electron density structure changes during the solar storm, electron density profiles derived from GPS measurements onboard the LEO satellite COSMIC (Constellation Observing System for Meteorology, Ionosphere, and Climate) are used. Whereas the ground based GPS measurements show horizontal distribution during the solar storm, the space based GPS measurements show a vertical distribution. Meanwhile, with consideration of the solar and geomagnetic parameter, the ionospheric anomallies with phenomenon of TEC and electron density profiles changes in the special region during the sun storm are analyzed in detail and discussed by adopting the numerical computions.

Keywords Ionosphere · GPS · COSMIC · TEC · VTEC · Kalman filter · GPS instrumental biases

H. Wang (✉) · Q. Wang · Y. Cheng
Chinese Academy of Surveying and Mapping, Beijing 10083, China
e-mail: whxxf82@126.com; wanghutongji@qq.com

J. Sun et al. (eds.), *China Satellite Navigation Conference (CSNC) 2013 Proceedings*, Lecture Notes in Electrical Engineering 243,
DOI: 10.1007/978-3-642-37398-5_5, © Springer-Verlag Berlin Heidelberg 2013

5.1 Introduction

A fierce solar flare erupted and triggered a coronal mass ejection on 1st August 2010, then just like large clouds of charged particles from the Sun hit against the Earth on 3 and 4th August 2010. As the particles zoomed along the magnetic field, they collided with and energized oxygen and nitrogen in the atmosphere. When the energized atoms relaxed, they emitted light, providing a brilliant show. Due to the solar flare occur, the Sun also sent a coronal mass ejection, a stream of charged particles towards the Earth about at the same time. It was reported that these clouds of particles had moved away toward the Earth at more than 1,600 km per second, and moved more quickly than any other coronal mass ejection in recently years. The Sun, interplanetary and the Earth were shown in the Fig. 5.1. As usual a flare is defined as a sudden, rapid, and intense variation in brightness. When magnetic energy that has built up in the solar atmosphere is suddenly released, a solar flare will occur. Radiation is emitted across nearly the entire electromagnetic spectrum, from radio waves at the long wavelength end, through optical emission to x-rays and gamma rays at the short wavelength end. The amount of energy released is the equivalent of millions of 100 megaton hydrogen bombs exploding at the same time. These particles will cause geomagnetic storm, ionospheric anomaly, radio communications loss and so on.

This solar storm also caused geomagnetic storm and sudden, unusual ionospheric variations. So this Solar storm provided a good opportunity for studying sun storm, geomagnetic storm, the ionospheric variations associated with the

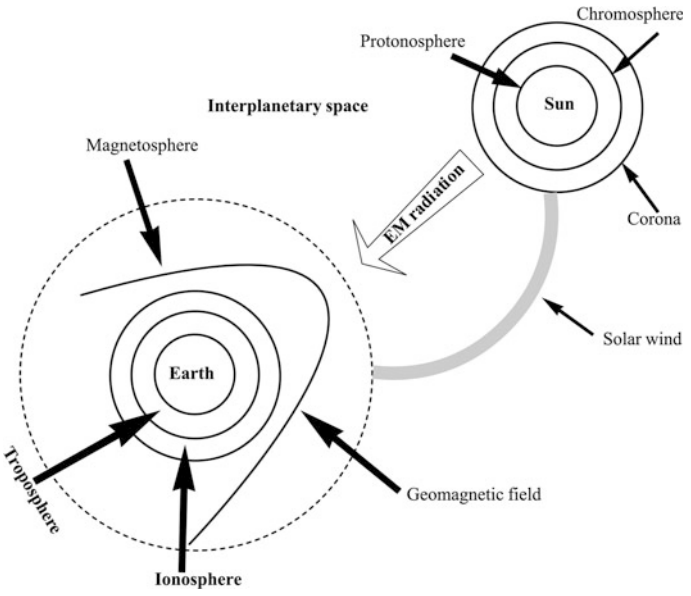

Fig. 5.1 Sun–Earth weather environment

photochemistry process and transportation process in the ionosphere and relationships to one another. It is well known that the solar storm may profoundly affect geomagnetic activity and the global ionosphere, inducing greater variations in geomagnetic parameters such as Kp index, Dst index, TEC (the total electron content), electron density distribution. Meanwhile these changes intensity will vary with latitude, longitude, local time and solar activity. So it is valuable and significant to study ionospheric variations during storm. The ionospheric changes can be monitoring by various techniques, such as ionosondes [1], incoherent scatter (ISR) [2], HF doppler, satellite beacon. On the one hand, these instruments are expensive and limited at a little area, secondly these instruments can't permanent and real-time monitor ionosphere without interval. Real-time monitoring of ionosphere changes using ground based GPS have been proven to be a powerful tool for investigating ionosphereic structure, mainly during suddenly ionosphere changes limited periods, when dynamics and energy dissipation process become extremely complex, such as geomagnetic storm [3], solar eclipse [4], earthquake [3], and so on. Meanwhile innovative space based GPS techniques have been developed in recent years. Due to occultation rise and set, COSMIC (Constellation Observing System for Meteorology, Ionosphere, and Climate) radio occultation technique can provide approximately 2,500 soundings of the ionosphere data per day which evenly distributed over the global regions. COSMIC has been demonstrated as a sounding the global ionosphere instrument more economically and effectively. Previous investigation by Lei et al. [5] verified that inversion algorithm of electron density profiles using COSMIC measurements is reliable, and their results are consistent with measurements from the ionosondes, ISR (incoherent scatter radars) and ionosphere forecast model (IRI). So electron density profiles retrieved from COSMIC measurements can be used for analyzing ionospheric variations.

The objective of this paper is to extend previous studies that ionospheric behavior during the solar storm was analyzed by combining with ground and space based GPS measurements. The organization of this paper is as follows: In Sect. 5.2, firstly, the algorithm based on the Kalman filter is proposed to obtain real-time estimation of TEC and GPS instrumental biases, due to a recursive estimator, the current measurements and the previous measurements can get the optimal estimator. Real-time and accurate TEC estimator can be calculated and the method can avoid influencing from the GPS instrumental biases. Secondly, ionospheric TEC rate were also proposed. In Sect. 5.3, we summarize the analytical about computation of ionosphere refraction error for GPS signals and also introduce the principle of inversion of electron density profiles from COSMIC occultation data. In Sect. 5.4, geomagnetic parameters are also discussed during the solar storm. Then the responses of the ground based GPS derived VTEC and TEC Rate over the Yangtze River Delta region are analyzed using the data from the Yangtze River Delta regional ground based GPS network. Following we show that during the solar storm electron density profiles from COSMIC measurements were compared with the quite days in the Yangtze River Delta region. Finally, conclusions of this paper are presented in Sect. 5.5.

5.2 Methodology of TEC Rate and TEC Derived from Ground Based GPS

5.2.1 TEC Rate Derived from Carrier Phase Data

TEC computed from the carrier phase is given as [6]:

$$TEC_{\Phi} = \frac{f_1^2 f_2^2[(\lambda_1\varphi_1 - \lambda_2\varphi_2) - (\lambda_1 N_1 - \lambda_2 N_2) - B]}{40.3(f_1^2 - f_2^2)} \tag{5.1}$$

where TEC_{Φ} is the TEC derived from carrier phase measurements; f is the carrier frequency; λ is the wave length; φ is the carrier phase; N is the integer ambiguity number; B is same as above. So the changes of TEC rate is as follow:

$$TECR_{\Phi}(t_{i+1}) = (TEC_{\Phi}(t_{i+1}) - TEC_{\Phi}(t_i))/(t_{i+1} - t_i) \tag{5.2}$$

where $TECR_{\Phi}(t_{i+1})$ is the TEC rate at epoch t_{i+1}.

5.2.2 TEC Derived from GPS

It is well known that TEC can be calculated using the differential pseudo range and carrier phase. However, the pseudo range derived TEC is corrupted by noise factors, such as multipath effects, measurement noise and GPS instrumental biases, et al. So the pseudo range derived TEC precision is lower than 5TECU. The carrier phase derived TEC is also corrupted by these factors. Due to the integer ambiguity number, the carrier phase derived TEC is not an absolute value. In order to deal with above drawbacks in TEC derived, we use a carrier phase-smoothed pseudo range technique where a new TEC estimates is derived from combining these measurements. In Hatch filter formula [7], Observation weight Q_i was established based on satellite elevation α_i, $Q_i = \sin\alpha_i$, $i = 1, 2, 3, \ldots$.

$$W_i = q_i / \sum_{k=1}^{i} q_k \tag{5.3}$$

The formula of a phase leveling technique is as follow:

$$\Delta\overline{P_i} = W_i \Delta P_i + (1 - W_i)[\Delta\overline{P_{i-1}} + (\Delta\Phi_i - \Delta\Phi_{i-1})] \tag{5.4}$$

In the above formula, we can only get TEC along the satellite transmission path. In order to get TEC over the GPS station region, we must build a ionospheric model to calculate. Commonly ionospheric models include curve polynomial fitting model, spherical harmonic model, generalized triangle model [8, 9]. In the paper, we employed curve polynomial fitting model. In the model, the ionosphere is approximated as a thin spherical shell located at a fixed height above the Earth's

surface. So each receiver-satellite link intersects the ionosphere exactly at one location, called ionospheric pierce point (IPP). The expression is as follow:

$$VTEC = TEC \cos Z^{'} \tag{5.5}$$

$$VTEC = \sum_{i=0}^{n} \sum_{j=0}^{m} E_{ij} (\varphi - \varphi_0)^i (S - S_0)^j + 9.52437 B \cos Z^{'} = 9.52437 \Delta \overline{P} \cos Z^{'} \tag{5.6}$$

where $(\varphi - \varphi_0)$ is the difference between the geomagnetic latitude of the IPP and the geomagnetic latitude of the receiver; $(S - S_0)$ is the difference the longitude of the IPP and the longitude of mean sun. B is GPS instruments biases; E_{ij} is coefficient; $\cos Z^{'}$ is the mapping function; $VTEC$ is the vertical total electron content.

In contrast with traditional least squares, the sequential Kalman filter provides a more accurate results as both the current and previous measurements is involved in the estimation process. Its process formula is as follow [10]:

$$\left.\begin{array}{ll} X_{k/k-1} = \Phi_{k/k-1} X_{k-1/k-1} & P_{k/k-1} = \Phi_{k/k-1} P_{k-1/k-1} \Phi_{k/k-1}^T + Q_k \\ X_{k/k} = X_{k/k-1} + K_k (Z_k - B_k X_{k.k-1}) & K_k = P_{k/k-1} B_k^T (B_k P_{k/k-1} B_k^T + R_k)^{-1} \\ P_{k/k} = (\mathrm{I} - K_k B_k) P_{k/k-1} & \end{array}\right\} \tag{5.7}$$

where X_k is the state vector; $\Phi_{k,k-1}$ is the state transition matrix; $P_{k/k-1}$ is the covariance matrix of state vector; Z_k is the observation vector; B_k is the observation matrix; K_k is the gain matrix; I is the identity matrix; R_k is the covariance matrix of measurement noises.

The unknown coefficients can be assumed to vary stochastically in time and approximated with a first order Gauss-Markov process. So the process noise of the white noise is given as:

$$q = \sigma^2 (1 - e^{-\frac{2\Delta t}{\tau}}) \tag{5.8}$$

where τ is correlation time; Δt is $t_{k+1} - t_k$; σ^2 is spectral density divided by $\frac{2}{\tau}$.

The expression of the transition matrix and the covariance matrix of the process noise are given as respectively:

$$\Phi = \begin{bmatrix} e^{-\frac{\Delta t}{\tau}} & & O \\ & \ddots & \\ & e^{-\frac{\Delta t}{\tau}} & \\ O & & \mathrm{I}_{nsat} \end{bmatrix}; \; Q = \begin{bmatrix} \sigma^2 (1 - e^{-\frac{2\Delta t}{\tau}}) & & & O \\ & \ddots & & \\ & & \sigma^2 (1 - e^{-\frac{2\Delta t}{\tau}}) & \\ O & & & O_{nsat} \end{bmatrix} \tag{5.9}$$

In the above equations, the satellite and receiver biases are assumed to remain constant with an identity transition matrix and zero process noise.

5.3 The Principle of Electron Density Retrieved from COSMIC Occultation Measurements

COSMIC is joint scientific mission between Taiwan and the USA, launched on 14 April 2006 with the goal of demonstrating the use of GPS radio occultation data in operational weather prediction, climate analysis, and space weather forecasting. The mission placed six small micro-satellites into six different orbits constellation at 700–800 km altitude and 30° separation in longitude between each satellite. Each COSMIC satellite is equipped with four antennas, so these satellites can receive signals from the USA GPS satellites. With the ability of performing both rising and setting occultation, COSMIC has been providing approximately 2,500 soundings of the ionosphere and atmosphere data per day, uniformly distributed around the globe since 2007. Especially, COSMIC data make a positive impact on particularly over region void of data such as oceans and polar region. Under the assumptions of spherical symmetry, straight-line propagation and electron density varies linearly with radius in between each level, electron density $N_e(r)$ was inverted by Lei et al. [5] as follows:

$$N_e(p_i) = c_{i,0}^{-1}\left[\frac{\bar{T}(p_i)}{p_i} - \sum_{k=1}^{m} c_{i,k} N_e(p_{i+k})\right] \tag{5.10}$$

where $c_{i,k}$ is a dimensionless coefficients, p_i is the distance from the Earth's center to the tangent point of a given straight line, $\bar{T}(p_i)$ is the calibrated TEC.

5.4 Results and Discussions

5.4.1 Geomagnetic Conditions

The Solar storm erupted and expelled large amount of energy and charged particles towards the Earth on 1st August 2010. Then these particles hit against the Earth and caused geomagnetic disturbance on 3rd and 4th August 2010. This disturbance was immediately identified by geomagnetic activity monitoring indices as seen in Figs. 5.2 and 5.3. The Dst index was obtained from the WDC for Geomagnetism, Kyoto. The Kp index was obtained from NOAA, USA. In the two figures show that the geomagnetic disturbance index Kp and Dst indicate twice major disturbances after the solar storm. The first geomagnetic disturbance started with the arrival of the shock at about 21:00UT on 3rd August 2010 and reached a minimum Dst value of −65nT at 24:00UT, accompanied with a maximum Kp index up to 6. Then the Dst index began to recover up to −23nT at 9:00UT, accompanied with a Kp index dropped to 3. However, second geomagnetic storm began, and subsequently the Dst index reached again −64nT at 20:00UT on

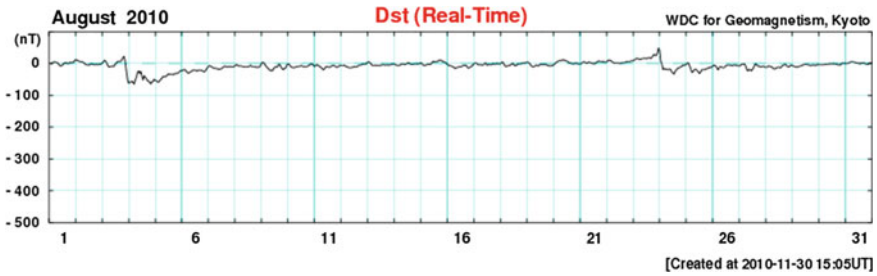

Fig. 5.2 The variation curve of DST 1st to 31th August 2010

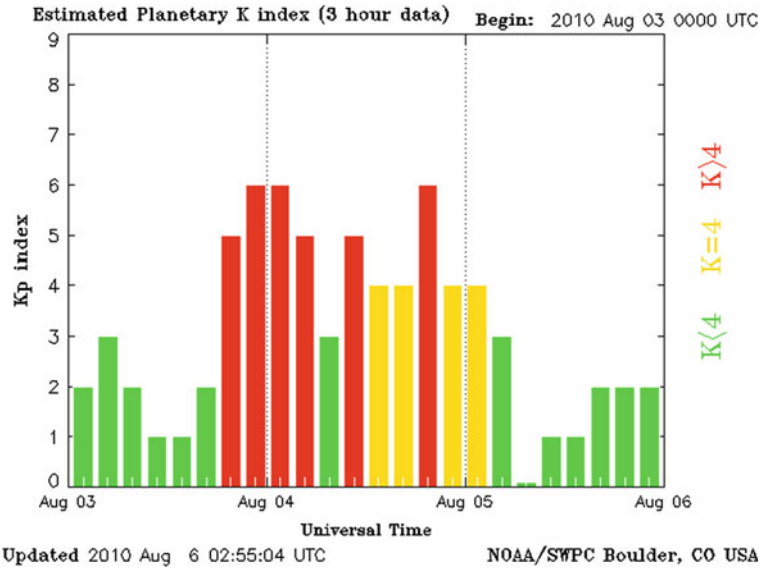

Fig. 5.3 The variation curve of KP index During 3rd 5th August 2010

4th August 2010, the Kp index also reached 6 at the same time. As can be seen from these indices, the geomagnetic activity returned to normal level on 7th August 2010.

5.4.2 Real-Time Monitoring of Ionosphere Changes Using Ground Based GPS Region Network

For this study, the ground based GPS region network measurements of the Yangtze River Delta regional GPS region network in China were used to produce real-time monitoring of *VTEC* changes and TEC rate (29th July to 7th August 2010).

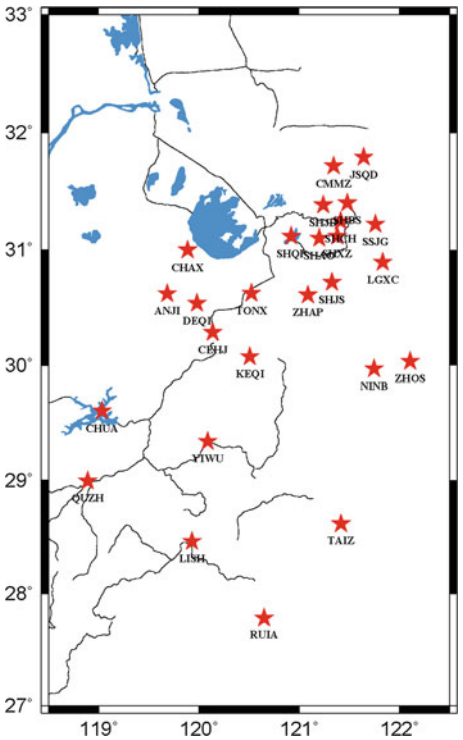

Fig. 5.4 Distribution of Shanghai regional GPS network, China

The regional GPS network consists of 26 permanent GPS sites (Fig. 5.4). In this solutions, we defined n and m value considering small region ($n = 3$; $m = 2$); in order to eliminate the multipath effects on GPS measurements, the minimum off elevation angle is selected at 15°; the ionospheric coefficients in (5.6) that describe the any point of *VTEC* above the monitoring region, and the GPS instruments biases. This solutions was proven to be robust with filter stabilizing after about one day [1, 4].

Using curve polynomial fitting model, we obtained the ionospheric coefficients, then calculated *VTEC* for GPS L1 signals above SHAO (IGS) site for a typical example. Figure 5.5 shows the diurnal variation of *VTEC* during 29th July to 7th August 2010. Before the solar storm erupted, the maximum of *VTEC* is about 22TECU in the daytime. Due to the solar storm began to erupted, more and more large amount of energy and charged particles hit against the Earth's atmosphere, the *VTEC* gradually increased, and reached the maximum value 42TECU at noon on 3rd August 2010. After this event, energetic particles receded, the maximum of *VTEC* recovered about 28TECU in the daytime. The minimum of *VTEC* on 3rd August 2010 was also bigger than other day. In a word, above the diurnal variation of *VTEC* can be due to the energy and charged particle precipitation induced by the solar wind collision with the Earth's atmosphere.

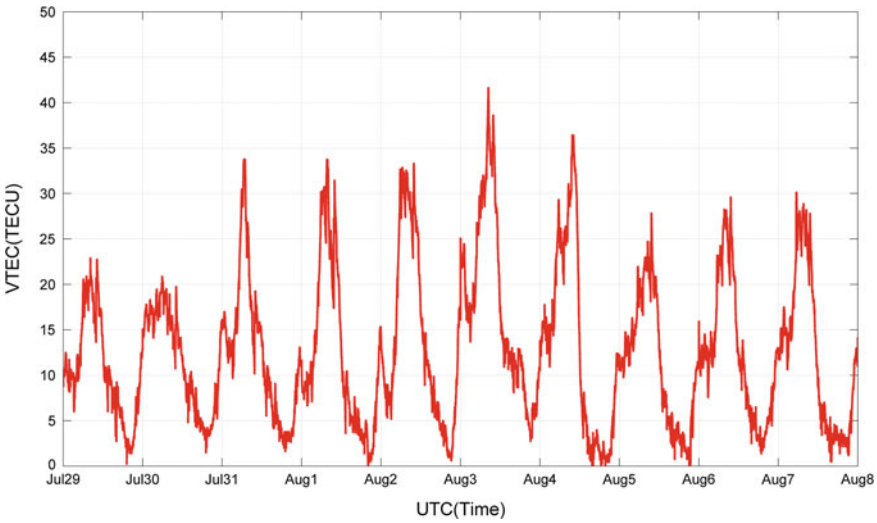

Fig. 5.5 The diurnal of *VTEC* variation during on 29th July to 7th August 2010 over SHAO (IGS) site

For the same typical example, Figs. 5.6 and 5.7 show the diurnal TEC rate changes on the two different days (29th July and 7th August, 2010) for all satellites observed (in different colors) at SHAO (IGS) site. Before the solar storm erupted, the TEC rates observed by all the satellites are below 0.02TECU/s using the 24-h data set on 29th July 2010. The TEC rate values changed relatively smoothly over the whole day period. When the energy and charged particles from the sun hit against the Earth's atmosphere, the TEC rate values changed very quickly, particularly between 4:00 and 16:00UT, showing strong variations of TEC. The maximum of TEC rate values is close to 0.05 TECU/s.

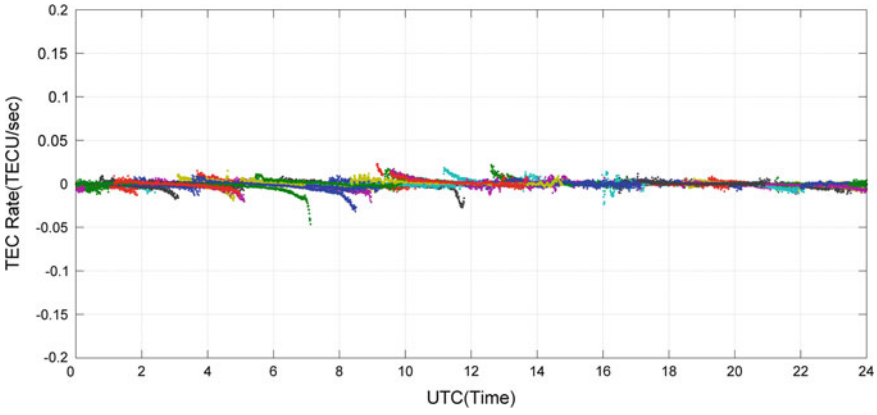

Fig. 5.6 TEC rate observed at SHAO (IGS) site on 29th July 2010

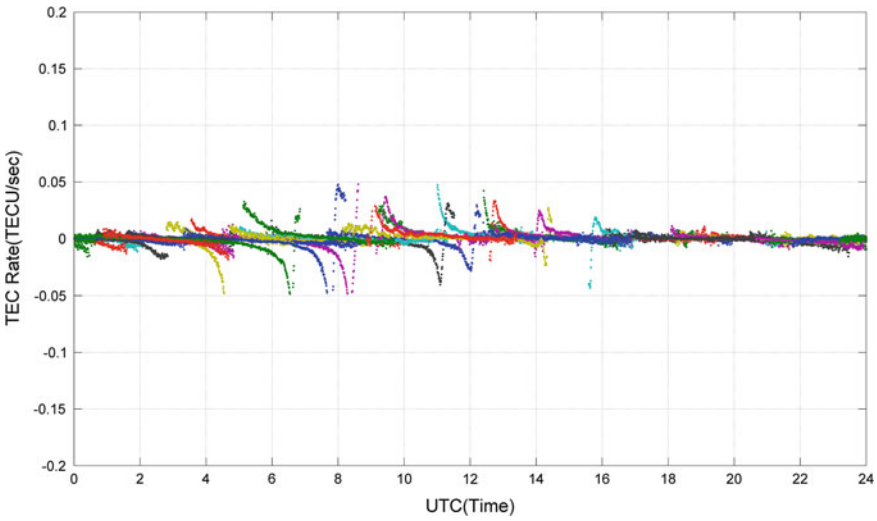

Fig. 5.7 TEC rate observed at SHAO (IGS) site on 3rd August 2010

5.4.3 Monitoring of Electron Density Profiles Changes Using Space Based GPS (COSMIC)

In this study we used electron density profiles from the COSMIC measurements. We selected coordinate of SHAO (IGS) site (31.01E, 121.20N) for examination and analysis in this study, because SHAO (IGS) site is located in the center of the Yangtze River Delta region. Positions of SHAO (IGS) site is shown in Figures with red pentacles (shown in Fig. 5.4). It is worth mentioning here that it is very difficult to find a radio occultation event that happens near any geographic location on the earth. So it should be noted that COSMIC measurements with tangent point at the at the F_2 peak height within 1 h, 5° latitude and 5° longitude at SHAO (IGS) site was selected [5, 11]. Electron density profiles of the quiet day on 29th to 30th July 2010 (according to day of 2010 year, from day 210 to 211) were compared with that of the solar storm day on 3rd to 4th August 2010 (according to day of 2010 year, from day 215 to 216).

Figure 5.8 indicates compared results at the similar time nearby SHAO (IGS) site. Since the solar storm expelled large amount of energy and charged particles towards the Earth, following happening the photochemistry process and transportation process in the ionosphere, and causing geomagnetic storm. It can be markedly seen that the electron density profiles at solar storm time featured considerably larger NmF2 and hmF2 than that at quiet time. It can be deduced that the influence from the solar storm is bigger than that from any other. It is noted that below 200 km the retrieved electron density in Fig. 5.8 become slightly inaccuracy, which is presumably a result of the horizontal gradients and the assumption of spherical symmetry in the retrieval [5].

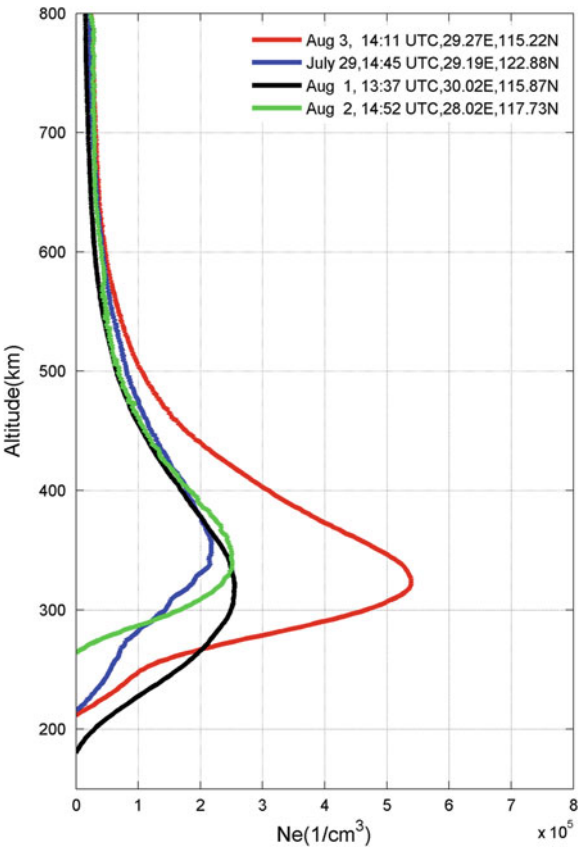

Fig. 5.8 Comparison of the COSMIC electron density profiles near IGS SHAO site

5.5 Conclusions

In this paper, we present the results of the solar storm, following the twice geomagnetic storms on 29th July 7th August 2010. Firstly, using ground based GPS measurements, the topside ionoshperic thin shell is determined, Kalman filter is also employed in order to obtain accuracy ionospheric coefficients and successfully eliminate GPS instruments biases. The real-time variations of the ionosphere are analyzed as a time series of TEC and TEC rate maps. TEC and TEC rate during the solar storm are compared and discussed with the quiet days. Secondly, using space based GPS measurements (COSMIC), electron density profiles during the solar storm are also compared and analyzed with the quiet days. The results indicate that due to the solar storm expelled large amount of energy and charged particles towards the Earth, the complicated variations of photochemistry process and transportation process happened in the ionosphere, the magnitude of TEC, TEC rate, NmF2 and HmF2 ionospheric parameters value during the solar storm become significantly higher than the quiet days.

It is worth noted that Ground based GPS measurements provide the horizontal TEC information, Space based GPS measurements (COSMIC) provide the vertical electron density distribution information. So the combined use of Ground based GPS and Space based GPS measurements provide a unique opportunity to comprehensive monitor ionospheric changes on regional or global scale. Furthermore, with more and more ground based GPS and space based GPS instruments built, the global real-time ionosphereic changes will be monitored. It will make a great contribution to studying ionosphere configuration and characteristics under any specific environment.

Acknowledgments This research was supported by National Natural Science Foundation of China (grants 41174023 and 40974018) and Scientific Research Foundation of the state Human Ministry for returned overseas Chinese Scholars (1208). The authors would like to thank Data center of Shanghai regional GPS network of China for providing the ground-based GPS tracking station data and COSMIC Data Analysis and Archiving Center (CDAAC) for providing the COSMIC occultation measurements.

References

1. Anghel A, Astilean A (2008) Near real-time monitoring of Ionosphere using Dual Frequency GPS data in a Kalman filter approach. Control Eng Appl Inform 10(2):33–38
2. Lei J, Liu L, Wan W, Zhang S (2004) Modeling the behavior of ionosphere above Millstone Hill during the September 21–27, 1998 storm. J Atmos Solar Terr Phys 66:1093–1102
3. Karia SP, Pathak KN (2011) Change in refractivity of the atmosphere and large variation in TEC associated with some earthquakes observed from GPS receiver. Adv Space Res 47:867–876. doi:10.1016/j.asr.2010.09.019
4. Wang H, Jie-Xian W (2010) Real-time monitoring of ionosphere changes in the Yangtze River Delta region based on GPS technology during the total solar eclipse of 22 July 2009. Chinese J Geophy V54(7):1718–1726. doi:10.3969/j.issn.0001-5733.2011.07.004
5. Lei J et al (2007) Comparison of COSMIC ionospheric measurements with ground-based observations and model predictions: preliminary results. J Geophys Res 112:A07308. doi:10.1029/2006JA012240
6. Liu Z, Wu C (2009) Study of the ionospheric TEC rate in Hong Kong region and its GPS/GNSS application. CGPS Meeting, pp 12–129
7. Hatch R (1982) The synergism of GPS code and carrier measurements. In: Proceedings of the 3rd international geodetic symposium on satellite doppler positioning, vol 2, New Mexico, pp 1213–1232
8. Komjathy A, Langley RB (1996) An assessment of predicated and measured ionospheric total electron content using a regional GPS net work. In: Proceedings of the national technical meeting of the Institute Of Navigation, Santa Monica, CA, 22–24 Jan 22-24 1996,pp 615–624
9. Schaer S (1999) Mapping and predicting the earth's ionosphere using the global positioning system. Ph.D dissertation, Astronomical Institute, University of Berne, Switzerland, 25 March 1999
10. Gelb A (1974) Applied optima estimation. MIT Press, Cambridge
11. Jakowski N, Wehrenpfennig A, Heise S, Reigber C, Luhr H, Grunwaldt L, Meehan TK (2002) GPS radio occultation measurements of the ionosphere from CHAMP: early results. Geophys Res Lett 29(10):1457. doi:10.1029/2001GL014364